THE JOURNAL OF PHYSICAL CHEMISTRY Letters

LETTER

pubs.acs.org/JPCL

Non-Condon Effects in the One- and Two-Photon Absorption Spectra of the Green Fluorescent Protein

Eugene Kamarchik*[,†,‡] and Anna I. Krylov[†]

[†]Department of Chemistry, University of Southern California, Los Angeles, California 90089-0482, United States

[‡]C. L. Emerson Center for Scientific Computation, Department of Chemistry, Emory University, Atlanta, Georgia 30322, United States

Supporting Information

ABSTRACT: We report calculations of one and two photon absorption (OPA and TPA, respectively) spectra of the green fluorescent protein (GFP) chromophore using the double-harmonic parallel-mode approximation and including explicit dependence of the electronic transition moments on nuclear geometry. The non-Condon effects are found to be more significant for TPA resulting in a different shape of the spectra and a blue shift of 500 cm^{-1} of the TPA peak absorption relative to OPA. The computed shift is in excellent agreement with the experimentally observed 700 cm^{-1}.

SECTION: Biophysical Chemistry

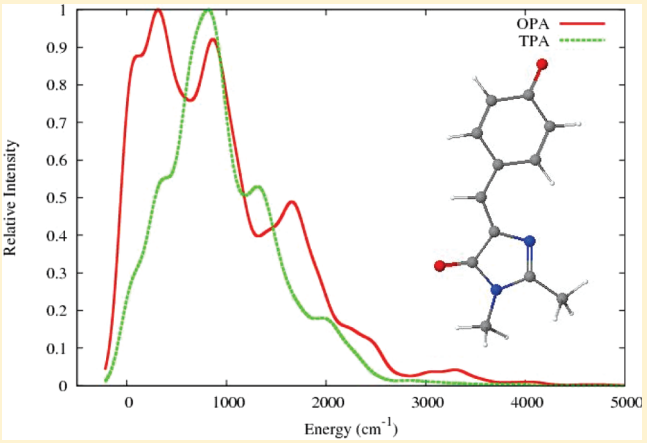

The green fluorescent protein (GFP) has revolutionized the fields of cell and molecular biology by permitting specifically targeted cellular imaging.[1−3] Recently, there has been considerable interest in using GFP in conjunction with two-photon laser scanning microscopy (TPLSM).[4−6] The longer wavelengths used in fluorescence imaging via two-photon excitation offer the advantages of greater penetration depth, reduced photodamage and photobleaching, and smaller background fluorescence. Two-photon absorption (TPA) experiments on GFP, however, have revealed a systematic blue shift of the absorption peak from one-photon absorption (OPA) experiments for which the cause is not fully understood.[7−12] Since there is also significant interest in the preparation of "designer" fluorescent proteins, which are capable of absorbing and emitting at specific wavelengths, an understanding of the factors that affect the TPA spectrum is important.

Several explanations for the observed 500−750 cm^{-1} shift of the absorption peak have been posited. One possible explanation is the presence of a nearby excited state that is dark under OPA, but bright for TPA.[7] Previous calculations in our group, however, show no evidence of a dark state in close proximity to the bright $\pi\rightarrow\pi^*$ state.[13,14] Moreover, the presence of a dark state within less than 1000 cm^{-1} from the bright state would result in strong vibronic couplings, intensity borrowing, and reduction in the fluorescence yield, which is not observed experimentally. Finally, as pointed out in refs 8 and 10, it is unlikely that such a dark state is present within the same energy interval from the bright state in many of fluorescent proteins (see, for example, ref 10) and in other molecules for which blue-shifted TPA spectra have been reported.[15]

An alternative explanation, which we pursue in this letter, is that the change in the transition moment along some normal coordinates leads to preferential transition into excited vibrational levels of the S_1 state. The transition of interest is $\pi\rightarrow\pi^*$, and a Huckel-like model predicts that the transition dipole moment depends sensitively on the geometry of the bridge moiety (see eq A4 in ref 16). Since a number of the Franck−Condon active modes involve stretching or bending around the central carbon atom of the chromophore, one can anticipate significant non-Condon effects for the absorption spectra. The vibronic effects in TPA absorption have been noted before[15] and suggested as a possible explanation of the blue-shifted TPA in fluorescent proteins,[10,11] however, no first-principle calculations have been performed to support this hypothesis.

This letter is organized as follows. In the next section we describe the details of how we compute the absorption spectra, including how we obtain geometries and OPA and TPA cross sections. The following section compares our calculated OPA spectra with gas-phase experiments[17] on the model chromophore and with wild-type GFP in the native protein environment.[7] We also compare our calculated OPA and TPA spectra. Finally we

Received: November 30, 2010
Accepted: January 30, 2011
Published: February 15, 2011

offer conclusions about the nature of the shift and the inherent sources of broadening for GFP.

The probability of a transition between two states is proportional to the square of the transition dipole matrix element between the initial (0) and final (f) states:

$$P_{0f} \propto \left[\int \Psi_0(\vec{r}_e,\vec{r}_N)\vec{\mu}\ \Psi_f(\vec{r}_e,\vec{r}_N)\ d\vec{r}_e\ d\vec{r}_N\right]^2 \quad (1)$$

where $\vec{\mu}$ is the electronic dipole moment operator, $\vec{r}_e$ and $\vec{r}_N$ are the electronic and nuclear coordinates, respectively, and $\Psi_0(\vec{r}_e,\vec{r}_N)$ and $\Psi_f(\vec{r}_e,\vec{r}_N)$ are the initial and final wave functions. Within the Born−Oppenheimer approximation, $\Psi_0(\vec{r}_e,\vec{r}_N)$ and $\Psi_f(\vec{r}_e,\vec{r}_N)$ are separated into electronic and nuclear parts such that

$$\Psi(\vec{r}_e,\vec{r}_N) \approx \psi^e(\vec{r}_e;\vec{r}_N)\phi^{vib}(\vec{r}_N) \quad (2)$$

where $\phi^{vib}(\vec{r}_N)$ is the vibrational wave function, and the dependence of $\psi^e(\vec{r}_e;\vec{r}_N)$ on the nuclear coordinates is parametric. Substituting this back into eq 1 gives

$$P_{0f} \propto \left[\int \psi_0^e(\vec{r}_e;\vec{r}_N)\phi_0^{vib}(\vec{r}_N)\vec{\mu}\ \psi_f^e(\vec{r}_e;\vec{r}_N)\phi_f^{vib}(\vec{r}_N)\ d\vec{r}_e\ d\vec{r}_N\right]^2 \quad (3)$$

Introducing the electronic transition moment,

$$\vec{\mu}_{0e}^{0f}(\vec{r}_N) = \int \phi_0^e(\vec{r}_e;\vec{r}_N)\vec{\mu}\ (\vec{r}_e)\phi_f^e(\vec{r}_e;\vec{r}_N)\ d\vec{r}_e \quad (4)$$

the final expression used for the transition probability is obtained as

$$P_{0f} \propto \left[\int \phi_0^{vib}(\vec{r}_N)\vec{\mu}_e^{0f}(\vec{r}_N)\phi_f^{vib}(\vec{r}_N)\ d\vec{r}_N\right]^2 \quad (5)$$

This expression takes into account both the spatial overlap of initial and final vibrational wave functions as well as the dependence of the transition moment on the nuclear geometry. In the Condon approximation, the dependence of μ^{0f} on nuclear coordinates is neglected, giving rise to familiar Franck−Condon factors (FCFs) defined as overlaps of vibrational wave functions of the initial and final states, $[\int \phi_0^{vib}(\vec{r}_N)\phi_f^{vib}(\vec{r}_N)\ d\vec{r}_N]^2$. As demonstrated in this letter, the inclusion of a transition moment with explicit dependence on the nuclear coordinates, i.e., non-Condon effects, can lead to both qualitative and quantitative changes in calculated spectra.

TPA is a nonlinear process, and the electronic factors that govern these transitions can be computed as second-order response properties.[18−20] The total probability of TPA can be described by an expression similar to eq 5 in which $\vec{\mu}_e^{0f}$ is replaced by the TPA transition moment, δ_{TPA}^{0f}:

$$\delta_{TPA}^{0f} = \frac{1}{15}\sum_{ij} S_{ii}^{0f}(S^{0f})_{jj}^* + 2S_{ij}^{0f}(S^{0f})_{ij}^* \quad (6)$$

where the indices i and j run over Cartesian coordinates, and S_{ij}^{0f} is the two-photon transition matrix element. The two-photon transition matrix element can itself be expressed as a sum over transitions between ground, $|0\rangle$, excited, $|n\rangle$, and final, $|f\rangle$, states:

$$S_{ij}^{0f} = \sum_n \left[\frac{\langle 0|\mu_i|n\rangle\langle n|\mu_j|f\rangle}{\omega_{0,n}-\omega} + \frac{\langle 0|\mu_j|n\rangle\langle n|\mu_i|f\rangle}{\omega_{0,n}-\omega}\right] \quad (7)$$

This sum runs over all excited states, and the excitation energy of the n^{th} excited state and the laser energy are given by $\omega_{0,n}$ and ω, respectively, while μ_i is the ith Cartesian component of the electronic dipole moment operator. Alternatively, the transition matrix elements may be computed directly from the second-order response, which is how they are obtained in this letter.

To compute FCFs and the total OPA and TPA transition probabilities (eq 5), we employ the double harmonic, parallel normal mode approximation and assume a linear dependence of the transition moments on the nuclear coordinates. The displacements along normal modes are computed using the ezSpectrum program,[21] and the optimized geometries of the ground and $\pi-\pi^*$ excited state are from ref 14. The normal modes of the ground-state are used in the parallel normal mode approximation. Previous calculations using ezSpectrum for polyatomic molecules (e.g., DNA bases) have demonstrated that the parallel normal mode approximation reproduces Franck−Condon envelopes well even in cases where there is significant mode mixing (Duschinsky rotation).[22]

For the model chromophore of GFP, we use 4′-hydroxybenzylidene-2,3-dimethylimidazoline (HBDI). The ground (S_0) state geometry and harmonic frequencies were previously optimized using resolution-of-the-identity second-order Møller−Plesset perturbation theory (RI-MP2), while the excited (S_1) state geometry was optimized using scaled-opposite-spin configuration interaction with single excitations and perturbative doubles [SOS-CIS(D_0)]. The displacements along normal modes connecting the S_0 and S_1 geometries were evaluated using the two previously calculated geometries and the S_0 normal modes. To obtain transition moments for OPA, CIS/cc-pVDZ calculations were performed at geometries where a single normal mode had been displaced from its equilibrium S_0 value to its S_1 value, where the value is the dimensionless scale factor along mass-weighted, normalized modes that yields the S_1 geometry. The calculations for the one-photon transition moments were performed using the Q-CHEM suite of quantum chemistry programs.[23]

TPA transition moments were obtained using the same displacements at the TD-DFT(B3LYP)/6-31G(d) level of theory in Dalton and assuming linear polarization of the light.[24] Although we report absolute TPA cross sections, we are primarily interested in the relative change of the TPA moments with molecular geometry. B3LYP significantly underestimates the absolute TPA cross-section for GFP, as reported previously; however, we expect that it reproduces well the correct dependence on geometry.[8] TPA calculations using the CIS wave functions yielded similar trends. To check for internal consistency we have also performed the same calculations using a ground (S_0) state optimized using B3LYP, and these are available in the Supporting Information (SI). In calculations of an isolated chromophore, it is necessary to use a small basis set to avoid mixing of the bright states with the electron-detached continuum,[13] which would normally be shifted to higher energies in a protein environment.

The full results of these calculations are shown in Table 1. Images showing the normal modes, absolute TPA cross sections computed using B3LYP and CIS, and additional details of the calculations are provided in the SI.

The gas-phase OPA spectrum of HBDI was calculated both with the Condon approximation and including non-Condon effects, and the two spectra are shown in Figure 1. The FCFs reveal several important vibrational progressions. The low frequency modes, ν_3, ν_9, ν_{11}, ν_{12}, and ν_{13}, contribute significantly to the overall broadening since their 0−1 transitions have intensity both by themselves and in combination with any other

dx.doi.org/10.1021/jz101616g |J. Phys. Chem. Lett. 2011, 2, 488–492

Table 1. Displacement of the Most Active Normal Coordinates (Calculated at the S_0 Equilibrium Geometry) for the S_1 State of the Deprotonated HBDI Anion[a]

mode	assignment	frequency (cm^{-1})	Δq	σ_{OPA}	σ_{TPA} (GM)
reference geometry				1.5959	2.8003
3	in-plane bend	79	−0.646	1.5902	2.5043
9	rock	203	0.183	1.6045	2.9221
11	stretch	246	0.298	1.5986	2.6691
12	stretch	273	−0.297	1.6133	2.3382
13	stretch	333	−0.221	1.5946	2.5552
19	out-of-plane bend	584	0.117	1.5867	2.6776
24	NCC bend	734	0.101	1.5885	2.2879
30	breathing	854	0.138	1.5614	3.0841
61	C═C stretch	1628	−0.066	1.5783	2.9221

[a] The frequencies and the calculated one- and two-photon cross sections are also shown for each displaced geometry. The displacements are given as dimensionless scale factors along mass-weighted, normalized normal modes.

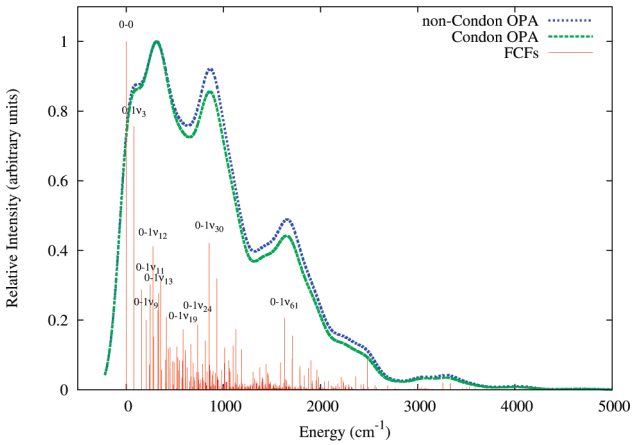

Figure 1. Stick spectrum representing the FCFs compared with the OPA spectrum within the Condon approximation and the OPA spectrum including the effect of changes in the transition dipole moment. Energy is given relative to the 0−0 adiabatic excitation energy.

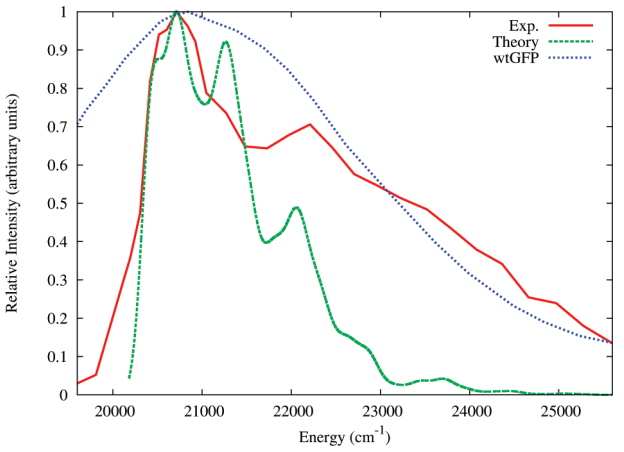

Figure 2. Comparison of calculated and experimental OPA for the deprotonated HBDI anion. The calculated spectrum has been convoluted with gaussians (100 cm^{-1} fwhm) and shifted so that the observed and calculated peak coincides. The OPA of wild-type GFP has also been shifted to match the peak positions so that the general shape of all three spectra can be compared.

Franck−Condon active mode. Although the 0−0 transition has the largest individual FCF, the higher density of peaks corresponding to combinations of low frequency modes in the region between 300 and 400 cm^{-1} serves to blue-shift the peak of the simulated spectrum (thus, in large molecules the peak maximum is likely to be blue-shifted relative to the vertical electronic energy difference, which should be kept in mind when comparing experimental spectra with electronic structure calculations). The full spectrum (i.e., including non-Condon effects) is also compared with the gas-phase experimental spectrum[17] obtained using the photodestruction technique, as shown in Figure 2. The calculated spectrum has been shifted so that the 0−0 adiabatic transition occurs at 20400 cm^{-1} allowing the calculated peak absorption to match the peak absorption of the experimental spectrum. Although not fully vibrationally resolved, the experimental spectrum contains features that agree with major features of the computed spectrum. For example, both spectra contain a peak (or shoulder) at approximately 21200 cm^{-1} and a peak at approximately 22100 cm^{-1}, which corresponds to the 0−1 transition in ν_{61} mode. The inclusion of non-Condon effects results in a small blue shift of the main peak by about 30 cm^{-1}, but does not appreciably change the overall structure.

The experimental spectrum loses intensity much slower than the calculated spectrum at higher energies, which could be due to either anharmonic effects (neglected in our simulations) or the incomplete deconvolution of the ionization and, especially, autoionization channels. Since the experimental spectrum is taken at 77 K, it may contain excitations in the low-frequency modes, which also contribute to the broadening. The comparison of the gas-phase action spectrum with the OPA absorption spectrum in the protein[7] reveals striking similarity in the peak shape, suggesting that the vibrational structure which leads to the broadening in the gas-phase is also present in the native protein. This strongly suggests that the difference between the computed and the experimental spectra is due to the anharmonic effects. Indeed, the calculations of the S_1 PES[14,25] reveal that the surface is rather flat in the Franck−Condon region, which should result in the apparent broadening of the FCF progression. Despite the similarity, however, the high-energy side of the gas-phase and protein spectra may experience broadening for different reasons, i.e., inhomogeneous broadening in the protein environment and ionization in the gas phase. With the exception of mode 19, the FC active modes are primarily in-plane motions, which should also be active in the protein environment, e.g., resonance Raman studies of the GFP and HBDI in solution have demonstrated that

dx.doi.org/10.1021/jz101616g | J. Phys. Chem. Lett. 2011, 2, 488–492

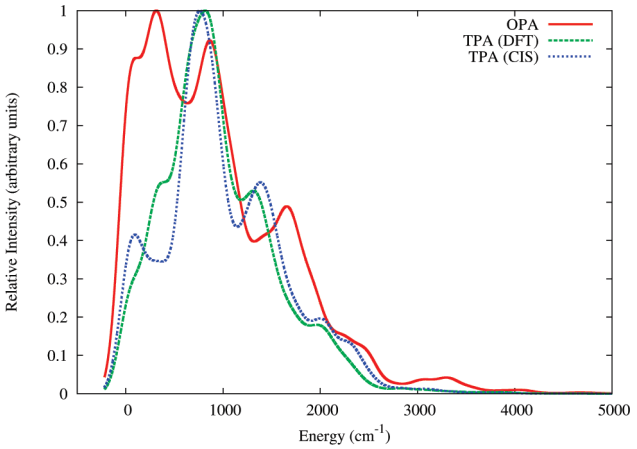

Figure 3. Comparison of OPA and TPA spectra for the deprotonated HBDI anion. The excitation energy is relative to the adiabatic 0−0 transition. Non-Condon effects blue shift the relative position of the TPA peak by approximately 500 cm^{-1}.

the stretching modes are not suppressed by the protein.[26] The important modes involve stretching or bending around the central carbon which leads to a distortion of the π-structure. As we have shown previously, a simple Hückel model offers some rational for the observed changes in both excitation energy and transition dipole.[16]

The inclusion of non-Condon effects in the TPA spectrum of HBDI, however, has a much more pronounced effect, which might be expected from the quadratic nature of the TPA matrix elements. This can already be seen from Table 1 where the maximum deviation of the one-photon cross-section from the reference value is 2.5%, whereas for the two-photon cross-section it is 18%. The comparison of the OPA spectrum with the TPA spectrum is shown in Figure 3. The net effect of including non-Condon effects in the TPA spectrum is an apparent blue shift of the peak absorption by approximately 500 cm^{-1}. This shift comes from preferential transition, which is enhanced by a favorable change in transition moment, to certain vibrationally excited modes of the S_1 state. This calculation indicates that the observed difference in peak position between OPA and TPA spectra in the gas phase is purely vibronic in nature, and does not require the presence of an additional "dark" state. In the protein, both OPA and TPA will be affected by the local environment; however, we believe that the underlying vibrational structure to both spectra should still be present. Since the blue TPA−OPA shift of a similar magnitude has been observed both in the protein environment and in the solution of the model chromophore (HBDI) in methanol,[7] it is reasonable to expect that the different dependence of the OPA and TPA electronic factors on the chromophore's geometry will not be eliminated by the interactions with the environment.

Because there is only a single bright low-energy transition, it is tempting to apply an effective two-state model to describe the observed spectra, such as those developed by Terenziani and co-workers.[27−30] These models, however, work best for compounds with well-defined charge symmetry such as donor−π-acceptor compounds because they make certain assumptions about the nature of the ground and excited states that do not apply in our case, i.e., due to an almost perfect resonance, the electronic structure of HBDI is of allylic type, and the $\pi\pi^*$ transition does not result in a charge-separated state.[13,16] Consequently, even the direction of the dipole moment change[13] in HBDI is perpendicular to the CCC moiety, contrary to the assumption of the Terenziani model that it is parallel to the molecular axis (as one would expect in donor−π-acceptor systems). Thus, it is not surprising that the TPA cross-section computed using eq 42 from ref 27 is several times smaller than the (already underestimated) B3LYP value. Additionally, these models do not account for the specific changes in the transition dipole moment that are precisely the reason for our observed blue shift.

In this letter we have presented the theoretical spectra for one- and two-photon absorption of the deprotonated HBDI anion computed using the double-harmonic parallel-mode approximation and including explicit dependence of the electronic transition moments on nuclear coordinates. The non-Condon effects result in a small blue shift (30 cm^{-1}) in OPA, and in a much larger shift (500 cm^{-1}) in TPA. These results suggest that the observed shift in the TPA peak position is most likely due to an increase in the transition moment along certain modes, which results in preferential transitions. Because there are nine FC active modes, the effect is not the result of a single enhancement but a collective result where certain transitions become weaker and certain transitions become stronger. As expected, however, the modes with significant enhancement are those involving distortions of the π-structure around the central carbon. The assignment of this shift to vibronic transitions agrees with recent calculations that have found no evidence for a nearby state that is only bright under two-photon absorption.[10−14] Our calculations suggest that the difference between OPA and TPA is purely vibronic in nature. In a future study, the effect of the protein environment of the Franck−Condon and the electronic factors of the cross sections will be investigated.

■ ASSOCIATED CONTENT

Supporting Information. Images of the Franck−Condon active normal modes and comparisons of the OPA and TPA calculations using different methods and basis sets. This material is available free of charge via the Internet at http://pubs.acs.org.

■ ACKNOWLEDGMENT

We are grateful to Dr. Ksenia Bravaya and Prof. Delmar Larsen for valuable discussions. This work is conducted under the auspices of the *iOpenShell* Center for Computational Studies of Electronic Structure and Spectroscopy of Open-Shell and Electronically Excited Species supported by the National Science Foundation through the CRIF:CRF CHE-0625419 + 0624602 + 0625237 and CHE-0951634 grants.

■ REFERENCES

(1) Tsien, R. Y. The Green Fluorescent Protein. *Annu. Rev. Biochem.* **1998**, *67*, 509.

(2) Zimmer, M. Green Fluorescent Protein (GFP): Applications, Structure, and Related Photophysical Behavior. *Chem. Rev.* **2002**, *102*, 759.

(3) Wang, Y.; Shyy, J.Y.-J.; Chien, S.; Chien, S. Fluorescence Proteins, Live-Cell Imaging, and Mechanobiology: Seeing is Believing. *Ann. Rev. Biomed. Eng.* **2008**, *10*, 1.

(4) Zipfel, W. R.; Williams, R. M.; Webb, W. W. Nonlinear Magic: Multiphoton Miscroscopy in the Biosciences. *Nat. Biotechnol.* **2003**, *21*, 1369.

(5) So, P. T. C.; Dong, C. Y.; Masters, B. R.; Berland, K. M. Two-Photon Excitation Fluorescence Microscopy. *Annu. Rev. Biomed. Eng.* **2000**, *2*, 399.
(6) Xu, C.; Zipfel, W.; Shear, J. B.; Williams, R. M.; Webb, W. W. Multiphoton Fluorescence Excitation: New Spectral Windows for Biological Nonlinear Microscopy. *Proc. Natl. Acad. Sci. U.S.A.* **1996**, *93*, 10763.
(7) Hosoi, H.; Ramaguchi, S.; Mizuno, H.; Miyawaki, A.; Tahara, T. Hidden Electronic Excited State of Enhanced Green Fluorescent Protein. *J. Phys. Chem. B* **2008**, *112*, 2761.
(8) Nifosi, R.; Luo, Y. Origin of the Anomalous Two-Photon Absorption in Fluorescent Protein DsRed. *J. Phys. Chem. B* **2007**, *111*, 505.
(9) Nifosi, R.; Luo, Y. Predictions of Novel Two-Photon Absorption Bands in Fluorescent Proteins. *J. Phys. Chem. B* **2007**, *111*, 14043.
(10) Drobizhev, M.; Tillo, S.; Makarov, N. S.; Hughes, T. E.; Rebane, A. Absolute Two-Photon Absorption Spectra and Two-Photon Brightness of Orange and Red Fluorescent Proteins. *J. Phys. Chem. B* **2009**, *113*, 855.
(11) Drobizhev, M.; Tillo, S.; Makarov, N. S.; Hughes, T. E.; Rebane, A. Absolute Two-Photon Absorption Spectra and Two-Photon Brightness of Orange and Red Fluorescent Proteins. *J. Phys. Chem. B* **2009**, *113*, 855.
(12) Blab, G. A; Lommerse, P. H. M; Cognet, L.; Harms, G. S; Schmid, T. Two-Photon Excitation Action Cross-Sections of the Autofluorescent Proteins. *Chem. Phys. Lett.* **2001**, *350*, 71.
(13) Epifanovsky, E.; Polyakov, I.; Grigorenko, B. L.; Nemukhin, A. V.; Krylov, A. I. Quantum Chemical Benchmark Studies of the Electronic Properties of the Green Fluorescent Protein Chromophore. 1. Electronically Excited and Ionized States of the Anionic Chromophore in the Gas Phase. *J. Chem. Theory Comput.* **2009**, *5*, 1895.
(14) Polyakov, I.; Grigorenko, B. L.; Epifanovsky, E.; Grigorenko, B. L.; Krylov, A. I.; Nemukhin, A. V. Potential Energy Landscape of the Electronic States of the GFP Chromophore in Different Protonation Forms: Electronic Transition Energies and Conical Intersections. *J. Chem. Theory Comput.* **2010**, *6*, 2377.
(15) Callis, P. R. Two-Photon-Induced Fluorescence. *Annu. Rev. Phys. Chem.* **1997**, *48*, 271.
(16) Epifanovsky, E.; Polyakov, I.; Grigorenko, B. L.; Nemukhin, A. V.; Krylov, A. I. The Effect of Oxidation on the Electronic Structure of the Green Fluorescent Protein Chromophore. *J. Chem. Phys.* **2010**, *132*, 115104.
(17) Forbes, M. W.; Jockusch, R. A. Deactivation Pathways of an Isolated Green Fluorescent Protein Model Chromophore Studied by Electronic Action Spectroscopy. *J. Am. Chem. Soc.* **2009**, *131*, 17038.
(18) Salek, P.; Vahtras, O.; Guo, J.; Luo, Y.; Helgaker, T.; Argen, H. Calculations of Two-Photon Absorption Cross Sections by Means of Density-Functional Theory. *Chem. Phys. Lett.* **2003**, *374*, 446.
(19) Tretiak, S. Resonant Nonlinear Polarizabilities in the Time-Dependent Density Functional Theory. *J. Chem. Phys.* **2003**, *119*, 8809.
(20) McClain, W. M. 2-Photon Molecular Spectroscopy. *Acc. Chem. Res.* **1974**, *7*, 129.
(21) Mozhayskiy, V. A.; Krylov, A. I.; ezSpectrum: http://iopenshell.usc.edu/downloads/.
(22) Bravaya, K. B.; Kostko, O.; Dolgikh, S.; Landau, A.; Ahmed, M.; Krylov, A. I. Electronic Structure and Spectroscopy of Nucleic Acid Bases: Ionization Energies, Ionization-Induced Structural Changes, and Photoelectron Spectra. *J. Phys. Chem. A* **2010**, *114*, 12305.
(23) Shao, Y.; Molnar, L. F.; Jung, Y.; Kussmann, J.; Ochsenfeld, C.; Brown, S.; Gilbert, A. T. B.; Slipchenko, L. V.; Levchenko, S. V.; O'Neil, D. P. Advances in Methods and Algorithms in a Modern Quantum Chemistry Program Package. *Phys. Chem. Chem. Phys.* **2006**, *8*, 3172.
(24) DALTON, a molecular electronic structure program, Release 2.0; see http://www.kjemi.uio.no/software/dalton/dalton.html, 2005.
(25) Olsen, S.; Smith, S. C. Bond Selection in the Photoisomerization Reaction of Anionic Green Fluorescent Protein and Kindling Fluorescent Protein Chromophore Models. *J. Am. Chem. Soc.* **2008**, *130*, 8677.
(26) Schellenberg, P.; Johnson, E.; Esposito, A. P.; Reid, P. J.; Parson, W. W. Resonance Raman Scattering by the Green Fluorescent Protein and an Analogue of Its Chromophore. *J. Phys. Chem. B* **2001**, *105*, 5316.
(27) Terenziani, F.; Katan, C.; Badaeva, E.; Tretiak, S.; Blanchard-Desce, M. Enhanced Two-Photon Absorption of Organic Chromophores: Theoretical and Experimental Assessments. *Adv. Mater.* **2008**, *20*, 4641.
(28) Terenziani, F.; Droumaguet, C.; Le ; Katan, C.; Mongin, O.; Blanchard-Desce, M. Effect of Branching on Two-Photon Absorption in Triphenylbenzene Derivatives. *Chem. Phys. Chem.* **2007**, *8*, 723.
(29) Terenziani, F.; Morone, M.; Gmouh, S.; Blanchard-Desce, M. Linear and Two-Photon Absorption Properties of Interacting Polar Chromophores: Standard and Unconventional Effects. *Chem. Phys. Chem.* **2006**, *7*, 685.
(30) Boldrini, B.; Cavalli, E.; Painelli, A.; Terenziani, F. Polar Dyes in Solution: A Joint Experimental and Theoretical Study of Absorption and Emission Band Shapes. *J. Phys. Chem. A* **2002**, *106*, 6286.